

# Schiff Base Functionalized 1,2,4-Triazole and Pyrene Derivatives for Selective and Sensitive Detection of $\text{Cu}^{2+}$ in the Mixed Organic- Aqueous Media

**Nam Gyu Choi**

Kongju National University

**Balasaheb D. Vanjare**

Kongju National University

**Prasad G. Mahajan**

Vidya Pratishtan Arts Science and Commerce College

**Rajendran Nagarajan**

Kongju National University

**Hyang Im Ryoo**

Kongju National University

**Ki Hwan Lee** (✉ [khlee@kongju.ac.kr](mailto:khlee@kongju.ac.kr))

Kongju National University <https://orcid.org/0000-0002-5553-4849>

---

## Research Article

**Keywords:** Schiff base functionalized 1,2,4-Triazole and Pyrene derivatives, chemosensor, copper sensing

**Posted Date:** June 7th, 2021

**DOI:** <https://doi.org/10.21203/rs.3.rs-534676/v1>

**License:**  This work is licensed under a Creative Commons Attribution 4.0 International License.

[Read Full License](#)

---

# Abstract

We have prepared Schiff base functionalized 1,2,4-Triazole and Pyrene derivatives for selective, sensitive, and naked eye colorimetric detection of  $\text{Cu}^{2+}$  in the mixed organic- aqueous media. Amongst the 18 different metal ions studied for absorption and fluorescence titration, only  $\text{Cu}^{2+}$  ion encourages the modification in spectral properties of Schiff base functionalized 1,2,4-Triazole and Pyrene Probe. The stoichiometric ratio of the Probe- $\text{Cu}^{2+}$  complex was determined to be 2:1 according to Job's plot. The lower detection limit estimated for  $\text{Cu}^{2+}$  is 0.234 nM which shows excellent sensitivity and selectivity of the present analytical method towards detection of  $\text{Cu}^{2+}$  ion in the mixed organic-aqueous media. The present approach has been successfully utilized for the quantitative determination of  $\text{Cu}^{2+}$  ion from environmental aqueous solution.

## 1. Introduction

Recently, studies on environmentally or biologically important metal ions have been continuously conducted. Many metal ions exist in nature and the human body, but not all metal ions have harmful effects. Some substances cause diseases, such as arsenic, cadmium, mercury, and lead[1], but there are also metal ions that are essential components of living things such as selenium, zinc, iron, and copper[2]. Of course, it is not good if there are many, but among them, copper is one of the metals used in the industry as a bronze alloy with tin since ancient times. It is also used in the general manufacturing industry and it is known as a corrosion-resistant metal. Due to this property, it is a metal mainly used as an electric wire. In biochemistry, it is used as a copper protein that plays a role in electron transport and oxygen movement[3]. The human body contains about 1.4 mg of copper per kilogram of body weight, and it is abundant in the brain, kidneys, and blood. It is also an essential component of hemoglobin, which carries oxygen. Besides, it is related to the behaving of p-type ATP and is necessary for promoting antioxidant function and for the action of some enzymes[4][5]. When a person's body is deficient in copper, copper deficiency creates or affects risk factors such as hypercholesterolemia and glucose tolerance, and can upsurge chronic irritation and oxidative stress, which are considered important triggers of cardiovascular disease[6]. However, on the contrary, copper toxicity is rare in humans but causes abdominal pain, liver and kidney failure, and death[7]. As such, copper is more important in industrially and environmentally.

Investigation for specific ions may be performed in various ways, such as electrically identifying ions[8] or using a membrane[9]. Among them, in this study, a chemosensor probe was used to observe the fluorescence intensity, that changes due to the photophysical properties that change through the reaction of an atom with an unshared electron pair in a molecule and a specific ion. Besides, many experiments for detecting specific ions of a chemical sensor using a change in the fluorescence spectrum, which are efficient in terms of cost, sensitivity, and selectivity, have been conducted[10][11][12]. Many compounds are being synthesized with chemistry-sensors, among the heterocyclic compounds, the 5 membered ring compound 4-Amino-1,2,4-Triazole-3-thiol derivative has an amine group and thiol group, so the amine

group reacts easily with aldehyde to become a Schiff base (Imine) group and can be used as a chemosensor. Schiff base is synthesized by simple experiments under simple conditions and is a good functional group for use in chemical sensors because of the simple structure of the double bond between nitrogen and carbon and the unshared electron pair of nitrogen[13]. In addition, there are more opportunities to bind with ions due to the sulfur in the thiol group. Pyrene is a generally well-known fluorophore, and as a remarkable feature, it is well known as a p-type quenching fluorophores, and due to its characteristic, many experiments have been conducted in the field of photophysical properties[14]. In this study, a Schiff Base derivative chemosensor probe **TP** or  $\text{Cu}^{2+}$  based on pyrene and imine was developed. However, the chemical sensor developed in this study was not a quenching type sensor, which is the main characteristics of pyrene, but an Off-On type sensor.

In summary, in this study, a Schiff base derivative (E)-5-(4-bromophenyl)-4-((pyren-1-ylmethylene)amino)-4H-1,2,4-triazole-3-thiol (**TP**) (Scheme 1) was synthesized, the structure was identified through nuclear magnetic resonance, infrared, and mass spectrometry, and various ions ( $\text{Na}^+$ ,  $\text{K}^+$ ,  $\text{Cs}^+$ ,  $\text{Cu}^+$ ,  $\text{Ca}^{2+}$ ,  $\text{Mg}^{2+}$ ,  $\text{Zn}^{2+}$ ,  $\text{Mn}^{2+}$ ,  $\text{Co}^{2+}$ ,  $\text{Pb}^{2+}$ ,  $\text{Ni}^{2+}$ ,  $\text{Cu}^{2+}$ ,  $\text{Fe}^{2+}$ ,  $\text{Hg}^{2+}$ ,  $\text{Cd}^{2+}$ ,  $\text{Ba}^{2+}$ ,  $\text{Fe}^{3+}$ ,  $\text{Y}^{3+}$ ) were analyzed using the photophysical properties analyzed with an ultraviolet-visible spectrophotometer and a fluorescence spectrophotometer in the mixed organic-aqueous media. The selectivity of the probe **TP** for detecting  $\text{Cu}^{2+}$  was confirmed, predicted how  $\text{Cu}^{2+}$  and the probe **TP** were bound, the binding ratio was checked, and the experiment in pH conditions carried out well and the lower detection limit of  $\text{Cu}^{2+}$  ion was confirmed through fluorescence measurement.

## 2. Synthesis

### 2.1 Reagents and instruments

Reagents, solvents, and metal cationic samples ( $\text{Na}^+$ ,  $\text{K}^+$ ,  $\text{Cs}^+$ ,  $\text{Cu}^+$ ,  $\text{Ca}^{2+}$ ,  $\text{Mg}^{2+}$ ,  $\text{Zn}^{2+}$ ,  $\text{Mn}^{2+}$ ,  $\text{Co}^{2+}$ ,  $\text{Pb}^{2+}$ ,  $\text{Ni}^{2+}$ ,  $\text{Cu}^{2+}$ ,  $\text{Fe}^{2+}$ ,  $\text{Hg}^{2+}$ ,  $\text{Cd}^{2+}$ ,  $\text{Ba}^{2+}$ ,  $\text{Fe}^{3+}$ ,  $\text{Y}^{3+}$ ) used for synthesis and binding experiment. It was prepared with chloride, nitrate, and sulfate salts, and each reagent was purchased from Alfa Aesar (UK), Sigma-Aldrich (Munich, Germany), Samjeon Pure Chemical Industries (Daejeon, Korea), and Daejeonghwageum (Siheung, Korea). These reagents used without further purification.  $^{13}\text{C}$  and  $^1\text{H}$  NMR were measured at 126 MHz, 500 MHz, and 400 MHz with a Bruker Avance (Germany) NMR Spectrophotometer using  $\text{DMSO-d}_6$ . Mass spectrometry (LC-MS) was measured using a 2975/ZQ2000 (waters) spectrometer. Infrared analysis was measured using a Frontier IR spectrophotometer (Perkin Elmer, USA). The process of the reaction was judged using TLC, and ultraviolet-visible absorption analysis was studied using a UV-2600 UV-Vis spectrophotometer of Shimadzu Corporation (Kyoto, Japan). Fluorescence analysis was measured using FluoroMate FS-2 from Scinco (Seoul, Korea).

### 2.2 Synthesis of ethyl 4-bromobenzoate **b**

4-bromobenzoic acid **a** (2.25 mmol) was added to ethanol with sulfuric acid and heated to 70-80°C for 5 hours. The progress of the reaction was confirmed by TLC. Thereafter, ethanol was obscure under

concentrated pressure, 100 ml of water was added to the residue, the reaction mixture was neutralized with sodium carbonate, and take out with ethyl acetate. The organic layer was removed with anhydrous sodium sulfate, and the solvent was evaporated under concentrated pressure to attain a solid product **b** (yield 83%). These were used as such in the next step without purification.

### 2.3 Synthesis of 4-bromobenzohydrazide **c**

Ethyl-4-bromobenzoate **b** (1.0 mmol) produced in the previous step was dissolved in ethanol, hydrazine hydrate (1.5 mmol) was added, and the mixture was refluxed for 5 hours. After completion of the reaction, ethanol was removed under reduced pressure, and the resulting solid was put in methanol and heated to dissolve it, and insoluble matter was filtered and stored in a fume hood for recrystallization. After recrystallization, a solid product **c** was obtained (yield 75%)

### 2.4 Synthesis of 4-amino-5-(4-bromophenyl)-4H-1,2,4-triazole-3-thiol **e**

4-bromobenzhydrazide **c** (1.0 mmol) was added to ethanol together with potassium hydroxide (1.5 mmol) and carbon disulfide (1.2 mmol), followed by stirring at 0 °C for 5 minutes. When the mixture was dissolved, diethyl ether was added thereto and filtered to obtain an intermediate salt **d**. Then, hydrazine hydrate (2.0 mmol) and distilled water were added and reacted overnight at 120 °C. After the reaction was completed, the reaction mixture was poured into distilled water (50 ml) and acidified with 5N HCl solution. Then, the resulting solid was filtered, washed with distilled water, stored in a fume hood for recrystallization, and dissolved in methanol. After recrystallization, a solid triazole intermediate product **e** was obtained (yield 90%). It was used as it is in the next step without purification.

### 2.5 Synthesis of (E)-5-(4-bromophenyl)-4-((pyren-1-ylmethylene)amino)-4H-1, 2, 4-triazole-3-thiol, TP

4-amino-5-(4-bromophenyl)-4H-1,2,4-triazole-3-thiol **e** (0.337 mmol) and 1-pyrenecarboxy-aldehyde (0.337 mmol) were added to methanol together with hydrochloric acid (2 drops) and reacted at 70° C for 3 hours. After completion of the reaction, the solid product was filtered and washed with ethanol, methanol and distilled water. After that, a dry and pure solid product **TP** was obtained (yield 90%).

#### (E)-5-(4-bromophenyl)-4-((pyren-1-ylmethylene)amino)-4H-1,2, 4-triazole-3-thiol (TP)

Yellow Solid; yield: 90%; <sup>1</sup>H NMR (500 MHz, DMSO-d<sub>6</sub>) δ 14.42 (s, 1H, SH), 10.91 (s, 1H, Imine CH), 8.74 (s, 1H, Ar), 8.69 – 8.66 (m, 1H, Ar), 8.47 – 8.40 (m, 4H, Ar), 8.38 (d, *J* = 8.9 Hz, 1H, Ar), 8.30 (d, *J* = 8.9 Hz, 1H, Ar), 8.18 (t, *J* = 7.6 Hz, 1H, Ar), 8.04 – 7.97 (m, 1H, Ar), 7.95 (d, *J* = 8.6 Hz, 2H, Ar), 7.81 (d, *J* = 8.6 Hz, 2H, Ar), 7.76 (d, *J* = 8.6 Hz, 1H, Ar). <sup>13</sup>C NMR (126 MHz, DMSO) δ 164.60, 162.46, 147.95, 133.82, 131.78, 130.60, 130.55, 130.29, 129.90, 129.73, 129.69, 127.28, 126.83, 126.77, 126.51, 125.32, 125.16, 124.74, 124.34, 124.32, 123.82, 123.36, 122.06. IR (KBr) 3098.96, 2927.63, 1907.86, 1740.51, 1624.75, 1592.96, 1573.90, 1535.62, 1497.98, 1422.23, 1397.63, 1375.87, 1320.02, 1303.63, 1272.79, 1258.45, 1234.21, 1184.89, 1165.36, 1139.68, 1108.18, 1072.05, 1013.18, 974.63, 901.95, 843.80, 820.18, 790.81, 766.89, 756.76, 733.10, 682.73cm<sup>-1</sup>; (ESI, m/z), 485.4 [M+2].

## 3. Analysis

### 3-1. Sample preparation

Probe **TP** was synthesized under relatively simple experimental conditions, but its solubility was limited at room temperature. It was not well soluble in methanol and ethanol, but relatively well soluble in DMSO, DMF, and THF. However, since DMSO has a high freezing point, it was limited to experiment in winter. Therefore, the probe **TP** was tested at a concentration of 1mM in a THF solvent. An analysis sample was prepared using THF and HEPES pH 7.4 buffer (THF: HEPES 8:2 v/v). And the prepared metal ions ( $\text{Na}^+$ ,  $\text{K}^+$ ,  $\text{Cs}^+$ ,  $\text{Cu}^+$ ,  $\text{Ca}^{2+}$ ,  $\text{Mg}^{2+}$ ,  $\text{Zn}^{2+}$ ,  $\text{Mn}^{2+}$ ,  $\text{Co}^{2+}$ ,  $\text{Pb}^{2+}$ ,  $\text{Ni}^{2+}$ ,  $\text{Cu}^{2+}$ ,  $\text{Fe}^{2+}$ ,  $\text{Hg}^{2+}$ ,  $\text{Cd}^{2+}$ ,  $\text{Ba}^{2+}$ ,  $\text{Fe}^{3+}$ ,  $\text{Y}^{3+}$ ) are all dissolved in distilled water. It was prepared at a concentration of 1 mM. In the case of copper ions, both monovalent cations and divalent cations were prepared, and in the case of monovalent cations, since they are insoluble in distilled water, a drop of HCl was added. Probe **TP** and metal cations were placed in the vial, mix well to react, and measured.

### 3-2. UV-Vis Absorption Spectroscopy

The probe TP and metal cation samples ( $\text{Na}^+$ ,  $\text{K}^+$ ,  $\text{Cs}^+$ ,  $\text{Cu}^+$ ,  $\text{Ca}^{2+}$ ,  $\text{Mg}^{2+}$ ,  $\text{Zn}^{2+}$ ,  $\text{Mn}^{2+}$ ,  $\text{Co}^{2+}$ ,  $\text{Pb}^{2+}$ ,  $\text{Ni}^{2+}$ ,  $\text{Cu}^{2+}$ ,  $\text{Fe}^{2+}$ ,  $\text{Hg}^{2+}$ ,  $\text{Cd}^{2+}$ ,  $\text{Ba}^{2+}$ ,  $\text{Fe}^{3+}$ ,  $\text{Y}^{3+}$ ) were prepared at room temperature. A 1 cm quartz cell was used, and the measurement range was measured from 200 nm to 700 nm. The maximum absorption wavelength of probe **TP** is 400 nm.

### 3-3. Fluorescence Spectroscopy

The approximate selectivity of TP towards metal ions was confirmed by the ultraviolet-visible absorption spectrum. Similarly, fluorescence intensity was also measured to confirm selectivity. The sample was measured using the same sample as in the absorption spectrum. The measurement starting wavelength of the fluorescence spectrum was 401 nm, and it was measured up to 700 nm. Also, 20  $\mu\text{M}$  of  $\text{Cu}^{2+}$  and other metal cations were added to 10  $\mu\text{M}$  of the probe **TP**, and the solvent was the same, and then the fluorescence intensity was measured to determine which ions preferentially react to the probe between  $\text{Cu}^{2+}$  and other metal ions. Also,  $\text{Cu}^{2+}$  was added to 10  $\mu\text{M}$  of probe **TP** from 1  $\mu\text{M}$  to 20  $\mu\text{M}$ , and the fluorescence intensity was measured, and the fluorescence intensity was measured again from 0.1  $\mu\text{M}$  to 2.0  $\mu\text{M}$ , and the lower detection limit was calculated. Then, using the same concentration (25  $\mu\text{M}$ ) of probe and copper(II) chloride solution, it makes a sample with a ratio of 1:9 ([Probe]:[ $\text{Cu}^{2+}$ ]) to 9:1 and measure the fluorescence intensity to analyze the binding ratio. Also, samples of pH 3 to pH 12 (HEPES buffer solution) were prepared and the fluorescence intensity was measured to determine the fluorescence intensity of each pH for  $\text{Cu}^{2+}$  ion with probe **TP**.

### 3-4. $^1\text{H}$ NMR Titration

To confirm the exact bonding position, a probe **TP** and copper(II) chloride solutions were prepared using the NMR solvent THF- $d_8$ . A sample containing probe **TP** was prepared, and the amount of  $\text{Cu}^{2+}$  in the

presence of probe TP was gradually increased, and six more samples were prepared to measure the  $^1\text{H}$  NMR titration.

## 4. Result

### 4-1. Selectivity

The colorimetric sensing ability of TP was investigated in THF: HEPES (8:2 v/v) upon the addition of a variety of metal ions. The probe TP with  $\text{Cu}^{2+}$  has a change in luminescence that can be distinguished from other ions with the naked eye through a UV lamp (365 nm). It confirmed that probe TP reacts selectively and preferentially to  $\text{Cu}^{2+}$  by using the ultraviolet-visible absorption spectrum and fluorescence emission spectrum. In the absorption spectrum,  $\text{Hg}^{2+}$  and  $\text{Cu}^{2+}$  in the presence of probe TP showed a slightly different shapes. In the case of  $\text{Hg}^{2+}$ , the absorption spectrum was generally shifted to the bathochromic shift. In the case of  $\text{Cu}^{2+}$ , the absorbance at 400 nm was significantly hypochromic shift (Fig. 1a.). On the other hand, the fluorescence intensity variation of probe TP towards various metal ions were evaluated systematically in THF: HEPES (8:2 v/v). The rest of the metal cations except for  $\text{Cu}^{2+}$  emitted an intensity similar to that of the probe TP (Fig. 1b). Therefore, when  $\text{Cu}^{2+}$  and other metal cations, respectively, towards probe TP were put together and measured and compared, it was found that the most of the copper ion preferentially reacts with probe TP. That is, the fluorescence emission intensity outcomes of the probe TP in the presence of each metal ions (blue pillars) and probe TP +  $\text{Cu}^{2+}$  ion in the presence of the other metal ions (orange pillars) as shown in Fig. 2. It means that  $\text{Cu}^{2+}$  preferentially combines with probe TP. In addition, considering that the fluorescence intensity increased by 5 times more than any other metal ions, it is thought that copper ion reacts preferentially. Evidently, the results demonstrated that probe TP exhibited high sensitivity and selectivity for  $\text{Cu}^{2+}$  in THF: HEPES (8:2 v/v).

### 4-2. Limited of Detection

The detection limit (LOD) is the minimum amount or minimum concentration that can detect an analyte contained in a sample. The calculation formula for the detection limit is

$$LOD = \frac{3.3\sigma}{K}$$

Where  $\sigma$  means the standard deviation of the response or signal, and K is the slope of the calibration curve.

Therefore, to calculate the detection limit for  $\text{Cu}^{2+}$  of probe **TP**,  $\text{Cu}^{2+}$  was added to 1-20  $\mu\text{M}$  in probe **TP** (10  $\mu\text{M}$ ) and fluorescence intensity was measured. However, only samples up to 1~2  $\mu\text{M}$  showed an increase in fluorescence, and 3  $\mu\text{M}$  samples showed similar fluorescence intensity (Fig. 3). Therefore, it has adjusted the concentration range and then it measured again to 0.1-1.9  $\mu\text{M}$  (Fig. 4). The fitting curve of fluorescence intensity of the probe **TP** with  $\text{Cu}^{2+}$ (0.1-1.9  $\mu\text{M}$ ) at 453.1 nm is shown as Fig. 5. The calculated detection limit is 0.234 nM.

**Table 1.** Comparison syntax between present method and already reported a method for detection of  $\text{Cu}^{2+}$ .

S. No.	Analysis method	Materials used	LOD	Reference
1	Fluorescence	Pyrene-based	0.87 nM	[12]
2	Colorimetric	Hexamethylbenzene-based	1.57 $\mu\text{M}$	[15]
3	Fluorescence	Peptide-based	54 nM	[16]
4	Colorimetric	Benzophenone-based	6.82 $\mu\text{M}$	[17]
5	Fluorescence	Triazole-based	12 nM	[18]
6	Colorimetric	Rhodamine 6G-based	1.0 $\mu\text{M}$	[19]
7	Colorimetric	1,5-Diphenylthiocarbazone-based	6.08, 6.21 $\mu\text{M}$	[20]
8	Colorimetric/ Fluorescence	quinoline-based	2.03 $\mu\text{M}$	[21]
9	Fluorescence	Triazole-pyrene-based	0.234 nM	<b>Our work</b>

When comparing the detection limit of the recently synthesized compound and the experimental method with the compound synthesized in this experiment, it can be seen that the detection limit belongs to the very lower side (**Table 1.**).

### 4-3. pH

Probe **TP** was tested at pH 7.4 (HEPES buffer solution). However, at different pHs, to determine which fluorescence intensity is exhibited by reacting to  $\text{Cu}^{2+}$  and to find an appropriate pH for detection, samples from pH 3 to pH 12 were prepared and fluorescence intensity was measured (Fig. 6). As a result, it shows low fluorescence intensity at acidic pH, moderate fluorescence at weakly basic pH than neutral, and better fluorescence intensity at weakly basic pH than neutral.

### 4-4. Binding

To confirm the binding method of probe **TP** and  $\text{Cu}^{2+}$ , Job's plot experiment,  $^1\text{H}$  NMR titration experiment, and mass analysis were performed[22]. Job's plot experiment is performed to find out the binding ratio of the two substances. Therefore, when the complex of probe **TP** and  $\text{Cu}^{2+}$  was formed, fluorescence spectra were measured with nine samples with different molar fractions to confirm the ratio of probe **TP** and  $\text{Cu}^{2+}$ (Fig. 7). A conversion point occurred in the sample with the mole fraction of probe **TP** 7. It can be seen from this result that the mole fraction of probe **TP** is 7 and  $\text{Cu}^{2+}$  is 3, and it can be seen that probe **TP** :  $\text{Cu}^{2+}$  has a binding ratio of 2:1.

Next, a  $^1\text{H}$  NMR titration experiment was performed to determine which functional group of probe **TP** reacts and binds with  $\text{Cu}^{2+}$  (Fig. 8).

When a small amount of copper(II) chloride solution was added to the probe **TP**, it was difficult to see the change of each peak, but as the amount of copper(II) chloride solution increased, the thiol peak near 13ppm moved to upfield. And it was shown that the imine hydrogen peak near 11.5ppm moved to the downfield as well. By the shift of each peak obtained through  $^1\text{H}$  NMR titration, it can be seen that the sulfur of the thiol group attached to the triazole ring and the nitrogen of the imine group interact with copper.

The modified Benesi-Hildebrand (B-H) equation was used to find the association constant ( $K_a$ ) between the probes **TP** and  $\text{Cu}^{2+}$ .

$$\frac{1}{F - F_0} = \frac{1}{(F_{MAX} - F_0)} + \frac{1}{K_a(F_{MAX} - F_0)} \frac{1}{[\text{Cu}^{2+}]^n}$$

Where,  $F_{max}$ ,  $F_0$ , and  $F$  are the fluorescence intensities of probe **TP** as maximum in the presence of  $\text{Cu}^{2+}$ , in absence of  $\text{Cu}^{2+}$ , and presence of  $\text{Cu}^{2+}$  at particular concentration i.e.  $[\text{Cu}^{2+}]$ , respectively. A 'n = 1' is the number of  $\text{Cu}^{2+}$  bound per probe **TP**. The association constant ( $K_a$ ) was calculated by drawing a Benesi-Hildebrand graph for the fluorescence intensity measured by putting the concentration of  $\text{Cu}^{2+}$  in the probe **TP** while increasing (Fig. 9). The larger the binding constant, the stronger the bonding strength between the probe and the ion, and less dissociation. The calculated binding constant is  $3.33 \times 10^5 \text{ M}^{-1}$ .

Through Job's plot experiment, it was found that probe **TP** and  $\text{Cu}^{2+}$  reacted 2:1, and through the  $^1\text{H}$  NMR titration experiment, it was found that sulfur of thiol group of probe **TP** and nitrogen of imine group are bound to  $\text{Cu}^{2+}$ . Based on the results obtained so far, the binding structure of probe **TP** and  $\text{Cu}^{2+}$  can be considered as follows (Fig. 10).

## 5. Conclusion

Probe **TP** can be easily synthesized under relatively simple reaction conditions. And the synthesized probe **TP** was confirmed using IR, NMR, and Mass Spectroscopy. When investigating the photophysical

properties, there was a limit to the solvent selection due to the nature of the pyrene derivative, but there were no major problems in experimenting. In the selectivity, the obtained results imply that the chemosensing mechanism is mainly the binding of Cu(II) by probe **TP** and formation of a probe **TP-Cu(II)** complex. The detection limit of Cu<sup>2+</sup> is 0.234 nM, and the probe **TP** and Cu<sup>2+</sup> were found to react at a ratio of 2:1 TP-Cu(II) complex. Through <sup>1</sup>H NMR, it was confirmed that the sulfur of the thiol group of probe **TP** and the nitrogen of the imine group and Cu<sup>2+</sup> were binded. Probe **TP** can used as a chemosensor for Cu<sup>2+</sup> due to its good sensitivity and sufficient selectivity for Cu<sup>2+</sup>, and further application experiments such as cytotoxicity experiments are possible.

## Declarations

### Credit Author Statements

Nam Gyu Choi has synthesized and characterized the compounds and prepared the manuscript; Balasaheb D. Vanjare and Prasad G. Mahajan have contributed to analysis; Rajendran Nagarajan has performed analysis with constructive discussion; Hyang Im Ryoo has contributed for photophysical measurements of compounds; Ki Hwan Lee has provided the idea and supervised the project.

**Ethical approval** Not applicable.

### Funding

This research was supported by Basic Science Research Program through the National Research Foundation of Korea (NRF) funded by the Ministry of Education (NRF- 2019R111A3A01059089)

### Data Availability

The data used to support the findings of this study are included within the article.

### Declaration of Competing Interest

The authors declare that there is no conflict of interest regarding the publication of this paper.

## References

1. L. Järup, Hazards of heavy metal contamination, Br. Med. Bull. 68 (2003) 167–182. <https://doi.org/10.1093/bmb/ldg032>.
2. A.T. Jan, M. Azam, K. Siddiqui, A. Ali, I. Choi, Q.M.R. Haq, Heavy metals and human health: Mechanistic insight into toxicity and counter defense system of antioxidants, Int. J. Mol. Sci. 16 (2015) 29592–29630. <https://doi.org/10.3390/ijms161226183>.
3. W. Kaim, J. Rall, Copper-A “Modern” Bioelement, (1996) 43–60.

4. M.C. Linder, M. Hazegh-Azam, Copper biochemistry and molecular biology., *Am. J. Clin. Nutr.* 63 (1996) 797S-811S. <https://doi.org/10.1093/ajcn/63.5.797>.
5. Y. Hatori, S. Lutsenko, The role of copper chaperone atox1 in coupling redox homeostasis to intracellular copper distribution, *Antioxidants*. 5 (2016) 1–16. <https://doi.org/10.3390/antiox5030025>.
6. J.J. Dinicolantonio, D. Mangano, J.H. O’Keefe, Copper deficiency may be a leading cause of ischaemic heart disease, *Open Hear.* 5 (2018) 1–8. <https://doi.org/10.1136/openhrt-2018-000784>.
7. M. Shike, Copper in Parenteral Nutrition, *Gastroenterology*. 137 (2009) S13–S17. <https://doi.org/10.1053/j.gastro.2009.08.017>.
8. H.H. Nejad, B. Ordoee, M. Khanmohammadi, A first principle photo-induced electron transfer study on a quinolin schiff base as Al<sup>3+</sup> chemosensor using TD-DFT method, *J. Mol. Struct.* 1196 (2019) 861–865. <https://doi.org/10.1016/j.molstruc.2019.01.004>.
9. X. Cui, T. Li, J. Li, Y. An, L. An, X. Zhang, Z. Zhang, A highly selective and reversible turn-off fluorescent chemosensor for Cu<sup>2+</sup> based on electrospun nanofibrous membrane modified with pyrenecarboxaldehyde, *Spectrochim. Acta - Part A Mol. Biomol. Spectrosc.* 207 (2019) 173–182. <https://doi.org/10.1016/j.saa.2018.09.021>.
10. S.Y. Lee, S.H. Lee, A Pyrenylboronic Acid-based Fluorescence Sensor for Highly Efficient Detection of Mercury(II) Ions, *J. Environ. Sci. Int.* 29 (2020) 201–207. <https://doi.org/10.5322/jesi.2020.29.2.201>.
11. S.D. Padghan, A.L. Puyad, R.S. Bhosale, S. V. Bhosale, S. V. Bhosale, A pyrene based fluorescent turn-on chemosensor: Aggregation-induced emission enhancement and application towards Fe<sup>3+</sup> and Fe<sup>2+</sup> recognition, *Photochem. Photobiol. Sci.* 16 (2017) 1591–1595. <https://doi.org/10.1039/c7pp00329c>.
12. D. Rajasekaran, K. Venkatachalam, V. Periasamy, “On–off–on” pyrene-based fluorescent chemosensor for the selective recognition of Cu<sup>2+</sup> and S<sup>2-</sup> ions and its utilization in live cell imaging, *Appl. Organomet. Chem.* 34 (2020) 1–9. <https://doi.org/10.1002/aoc.5342>.
13. M. Saleem, N.G. Choi, K.H. Lee, Facile synthesis of an optical sensor for CO<sub>3</sub><sup>2-</sup> and HCO<sub>3</sub><sup>-</sup> detection, *Int. J. Environ. Anal. Chem.* 95 (2015) 592–608. <https://doi.org/10.1080/03067319.2015.1046056>.
14. J. Wang, C.-S. Ha, Highly Sensitive and Selective Fluorescent Chemosensors Specific for Pd<sup>2+</sup> Detection, *Adhes. Interface.* 14 (2013) 13–20. <https://doi.org/10.17702/jai.2013.14.1.013>.
15. A. Kim, J.B. Chae, C.J. Rha, C. Kim, A colorimetric chemosensor for selective detection of copper ions, *Color. Technol.* 136 (2020) 459–467. <https://doi.org/10.1111/cote.12491>.
16. C. Hao, Y. Li, B. Fan, G. Zeng, D. Zhang, Z. Bian, J. Wu, A new peptide-based chemosensor for selective imaging of copper ion and hydrogen sulfide in living cells, *Microchem. J.* 154 (2020) 104658. <https://doi.org/10.1016/j.microc.2020.104658>.
17. D. Yun, J.B. Chae, C. Kim, A novel benzophenone-based colorimetric chemosensor for detecting Cu<sup>2+</sup> and F<sup>-</sup>, *J. Chem. Sci.* 131 (2019). <https://doi.org/10.1007/s12039-018-1585-2>.

18. A.N. Kursunlu, M. Ozmen, E. Güler, A Novel Fluorescent Chemosensor for cu (II) Ion: Click Synthesis of Dual-Bodipy Including the Triazole Groups and Bioimaging of Yeast Cells, *J. Fluoresc.* 29 (2019) 1321–1329. <https://doi.org/10.1007/s10895-019-02456-3>.
19. Q. Huang, Y.T. Chen, Y.W. Ren, Z.Y. Wang, Y.X. Zhu, Y. Zhang, A rapid and naked-eye visible rhodamine 6G-based chemosensor for sensitive detection of copper(ii) ions in aqueous solution, *Anal. Methods.* 10 (2018) 5731–5737. <https://doi.org/10.1039/c8ay02019a>.
20. E. Normay, R. Syuhada, H. Ismail, M.N. Ahmad, M.A. Yarmo, K.H.K. Bulat, Chemosensor development of Cu<sup>2+</sup> recognition using 1,5-diphenylthiocarbazone: Optimization, COSMO-RS and DFT studies, *J. Braz. Chem. Soc.* 30 (2019) 1850–1859. <https://doi.org/10.21577/0103-5053.20190095>.
21. A. Farhi, F. Firdaus, H. Saeed, A. Mujeeb, M. Shakir, M. Owais, A quinoline-based fluorescent probe for selective detection and real-time monitoring of copper ions-a differential colorimetric approach, *Photochem. Photobiol. Sci.* 18 (2019) 3008–3015. <https://doi.org/10.1039/c9pp00247b>.
22. M. Mabrouk, S.F. Hammad, M.A. Abdelaziz, F.R. Mansour, Ligand exchange method for determination of mole ratios of relatively weak metal complexes: A comparative study, *Chem. Cent. J.* 12 (2018) 1–7. <https://doi.org/10.1186/s13065-018-0512-4>.

## Figures

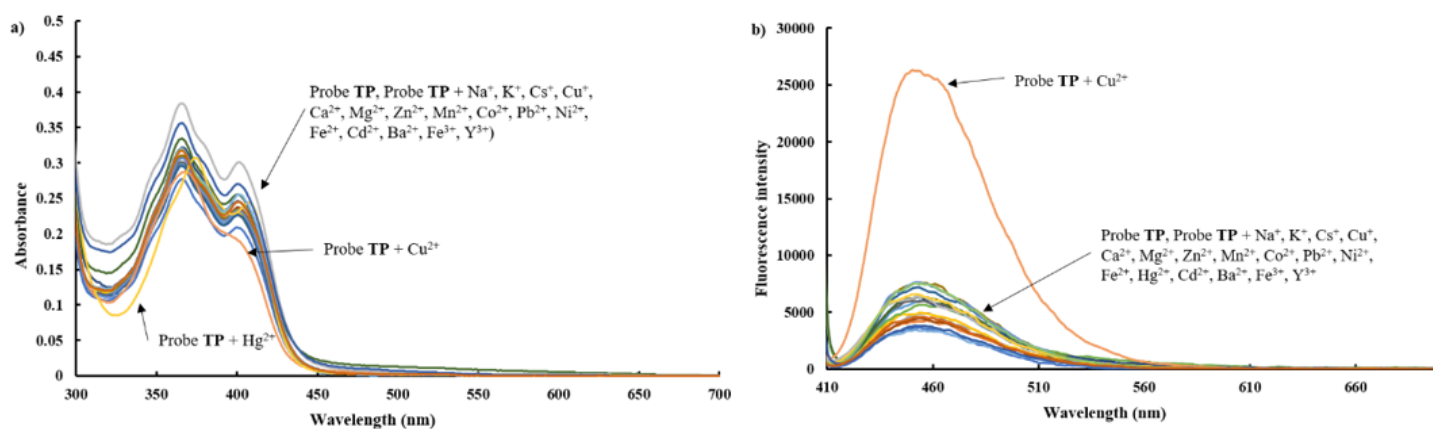


**Figure 1**

a) Absorption spectra of TP (10  $\mu\text{M}$ ) in the existence of various metal ions (Na<sup>+</sup>, K<sup>+</sup>, Cs<sup>+</sup>, Cu<sup>+</sup>, Ca<sup>2+</sup>, Mg<sup>2+</sup>, Zn<sup>2+</sup>, Mn<sup>2+</sup>, Co<sup>2+</sup>, Pb<sup>2+</sup>, Ni<sup>2+</sup>, Cu<sup>2+</sup>, Fe<sup>2+</sup>, Hg<sup>2+</sup>, Cd<sup>2+</sup>, Ba<sup>2+</sup>, Fe<sup>3+</sup>, Y<sup>3+</sup>) (20  $\mu\text{M}$ ) in THF:HEPES (pH 7.4) 8:2 (v/v). b) Fluorescence spectra of TP (10  $\mu\text{M}$ ) in the existence of various metal ions (20  $\mu\text{M}$ ) in THF:HEPES (pH 7.4) 8:2 (v/v).

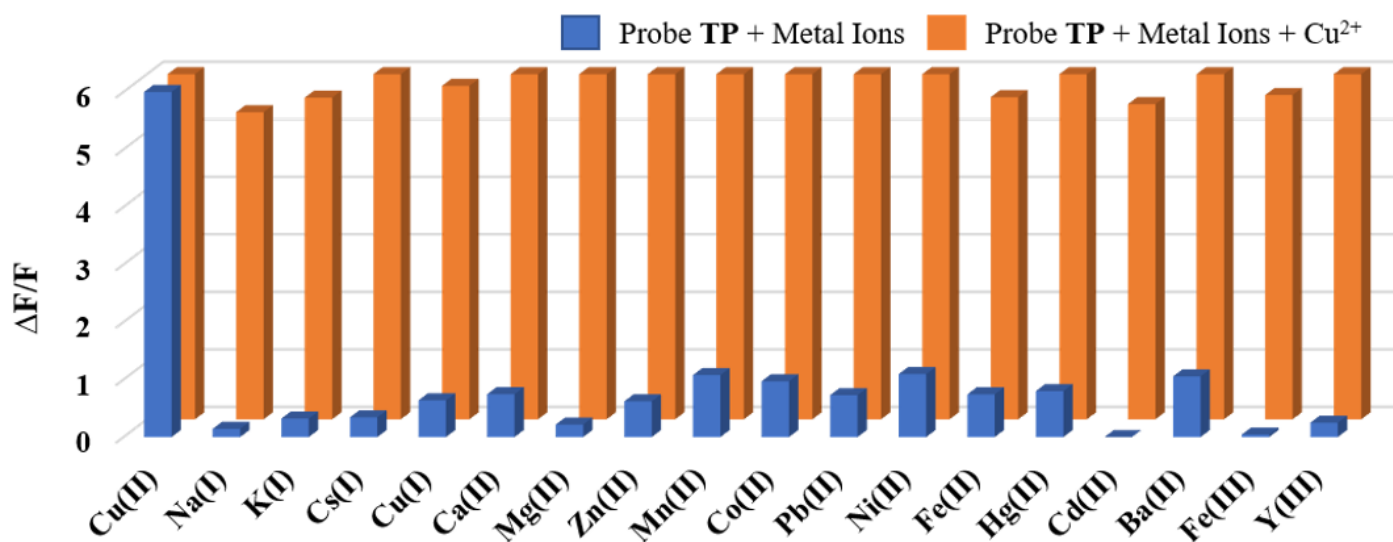


Figure 2

Competitive binding studies between Probe TP (10  $\mu\text{M}$ ) with various metal ions (Na<sup>+</sup>, K<sup>+</sup>, Cs<sup>+</sup>, Cu<sup>+</sup>, Ca<sup>2+</sup>, Mg<sup>2+</sup>, Zn<sup>2+</sup>, Mn<sup>2+</sup>, Co<sup>2+</sup>, Pb<sup>2+</sup>, Ni<sup>2+</sup>, Cu<sup>2+</sup>, Fe<sup>2+</sup>, Hg<sup>2+</sup>, Cd<sup>2+</sup>, Ba<sup>2+</sup>, Fe<sup>3+</sup>, Y<sup>3+</sup>) (20  $\mu\text{M}$ )

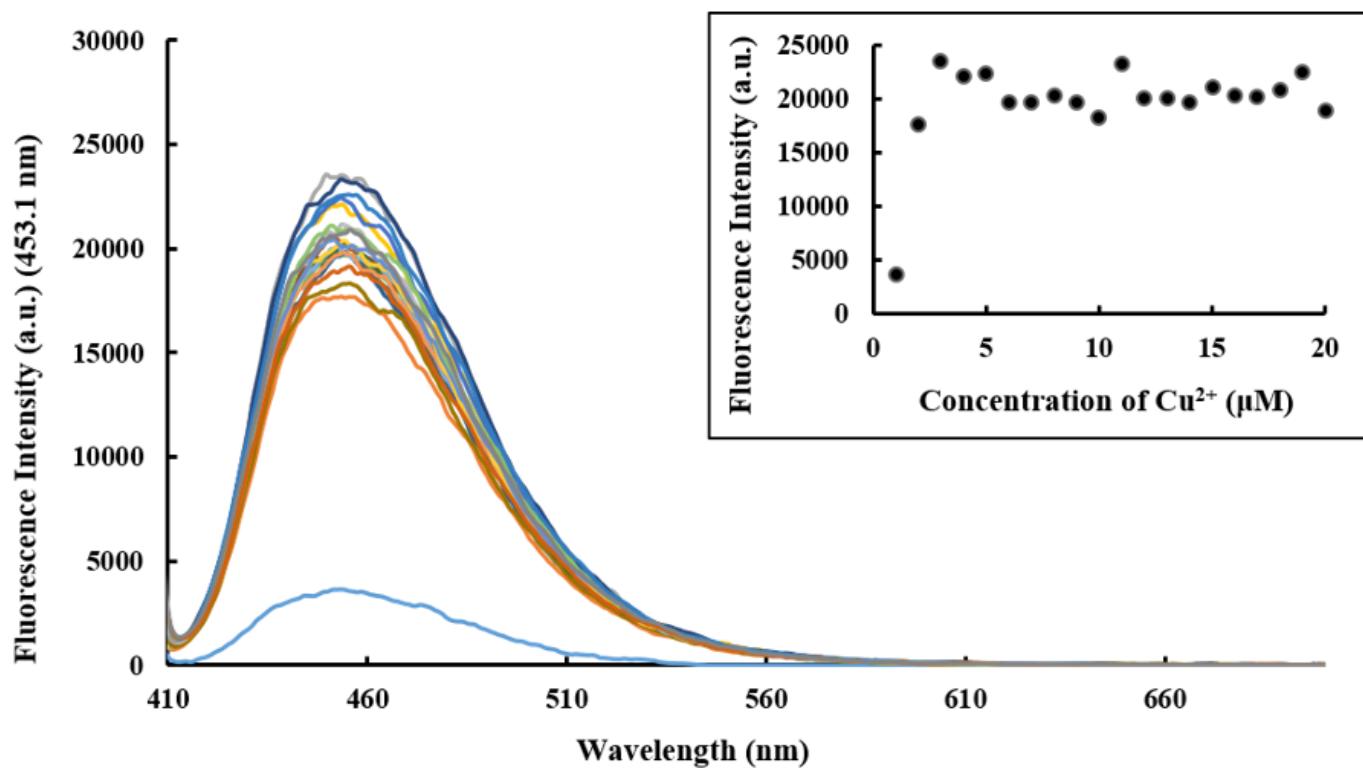


Figure 3

Fluorescence emission spectrum of each sample containing Cu<sup>2+</sup> up to 1  $\mu\text{M}$ -20  $\mu\text{M}$  in 10  $\mu\text{M}$  Probe TP.

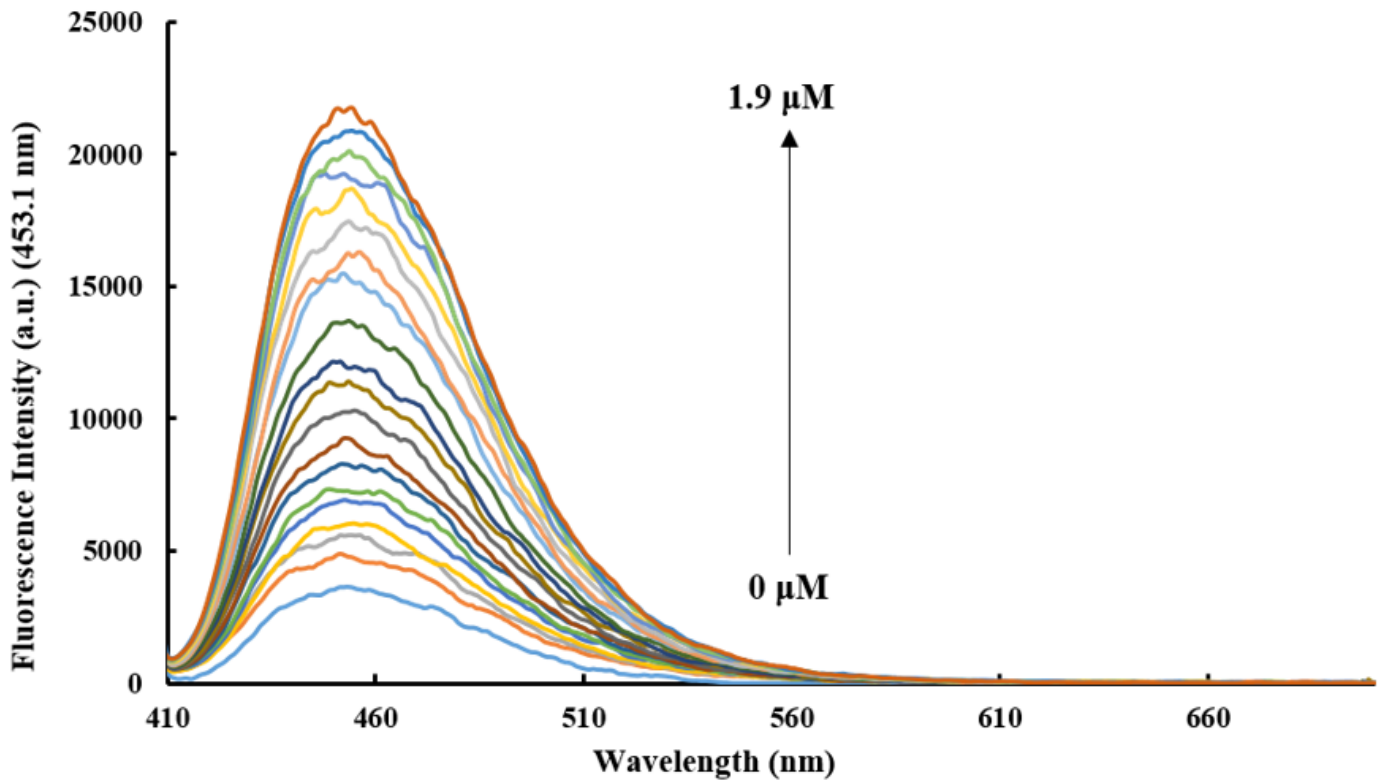
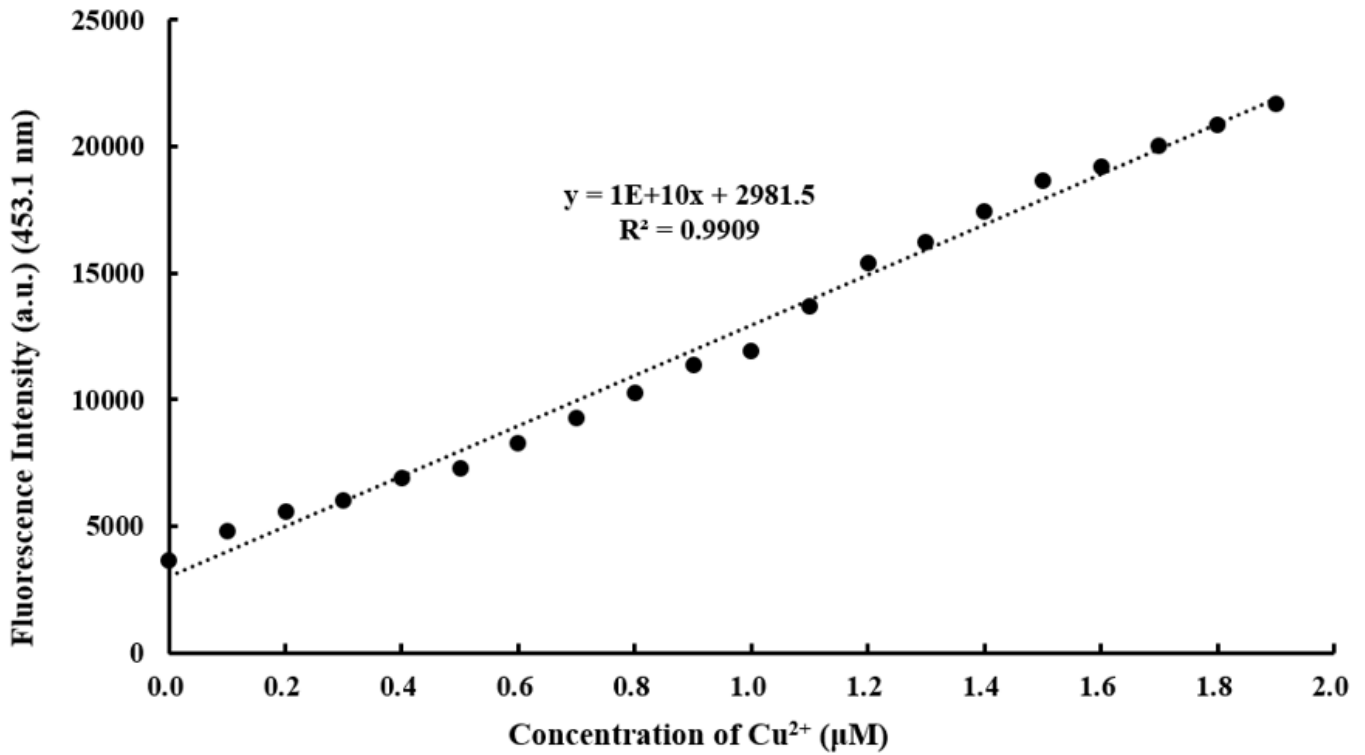


Figure 4

Fluorescence emission spectrum of each sample containing 0.1-1.9  $\mu\text{M}$   $\text{Cu}^{2+}$  in 10  $\mu\text{M}$  probe TP.



**Figure 5**

Fitting curve of fluorescence intensity of the chemosensor TP with  $\text{Cu}^{2+}$  (0.1-1.9  $\mu\text{M}$ ) at 453.1 nm

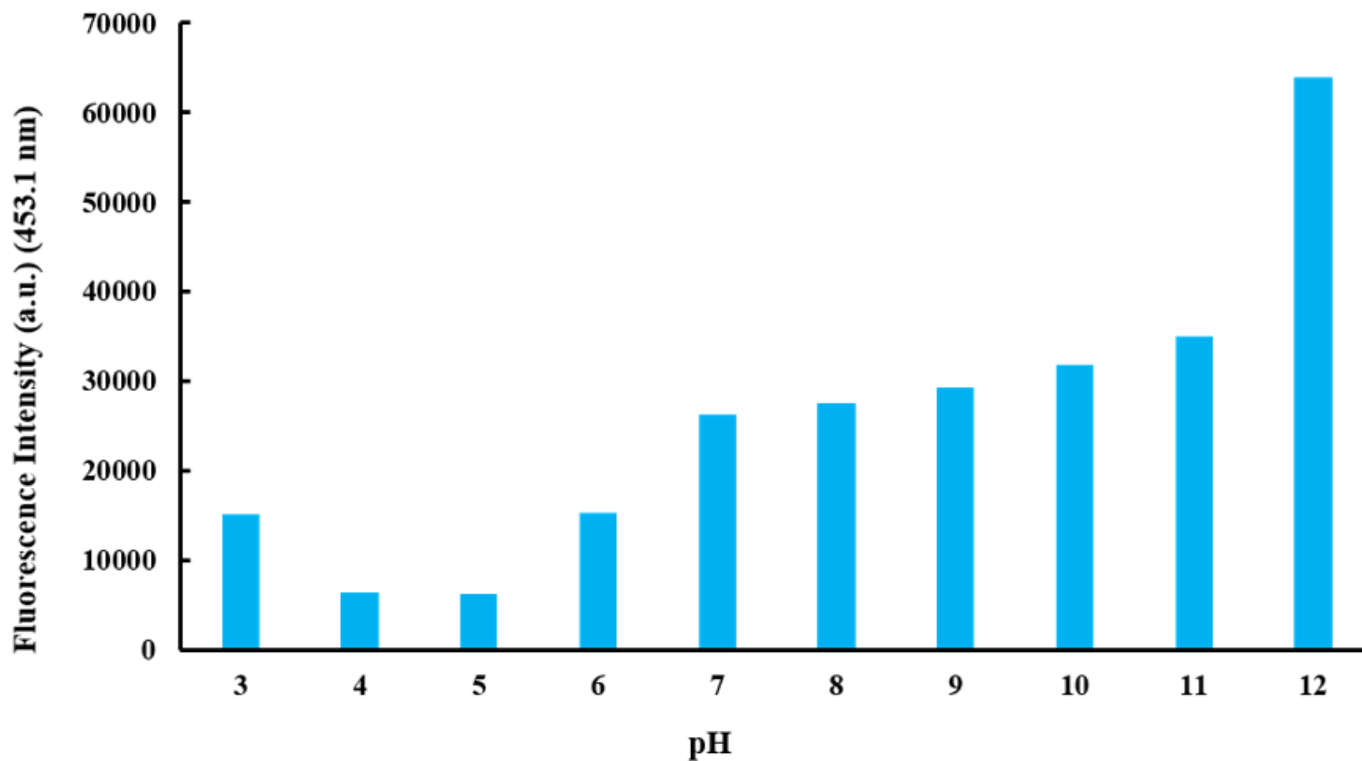


**Figure 6**

Fluorescence intensity of  $\text{Cu}^{2+}$  (20  $\mu\text{M}$ ) of probe TP (10  $\mu\text{M}$ ) measured using THF and each pH buffer (8:2 v/v) as a solvent.

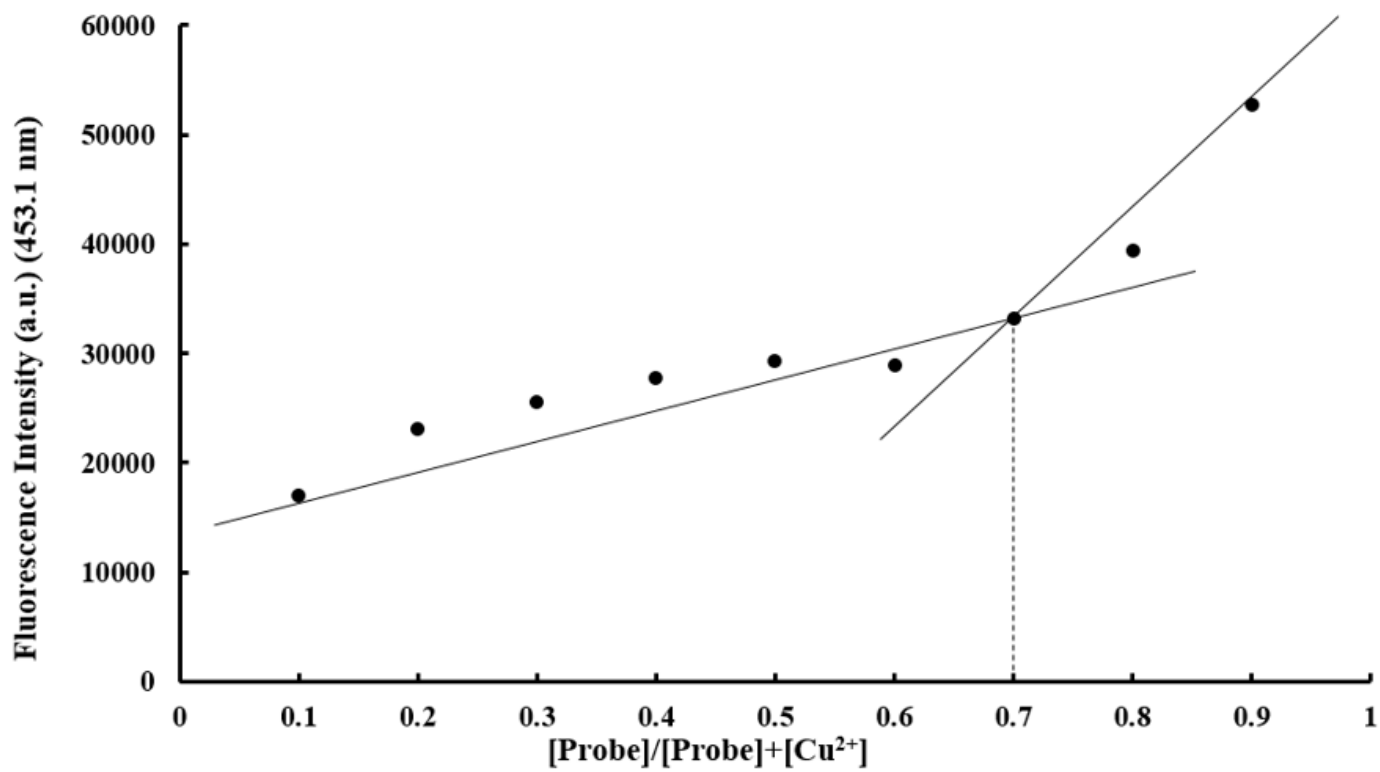
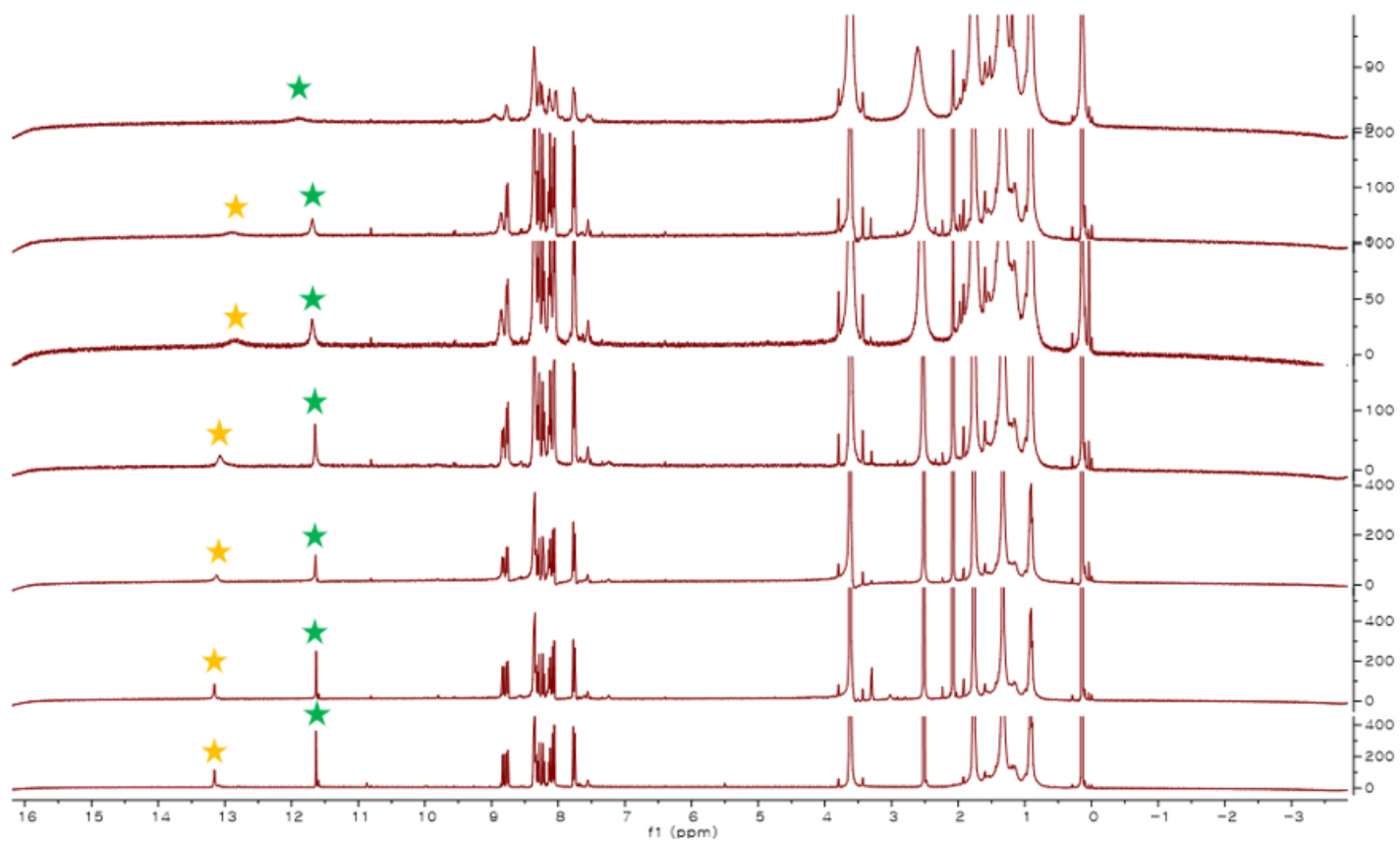


Figure 7

Job's plot for detecting the stoichiometry of probe:copper(II) complex according to the mole fraction of probe TP.



**Figure 8**

<sup>1</sup>H NMR titration spectrum for Cu<sup>2+</sup> of probe TP.

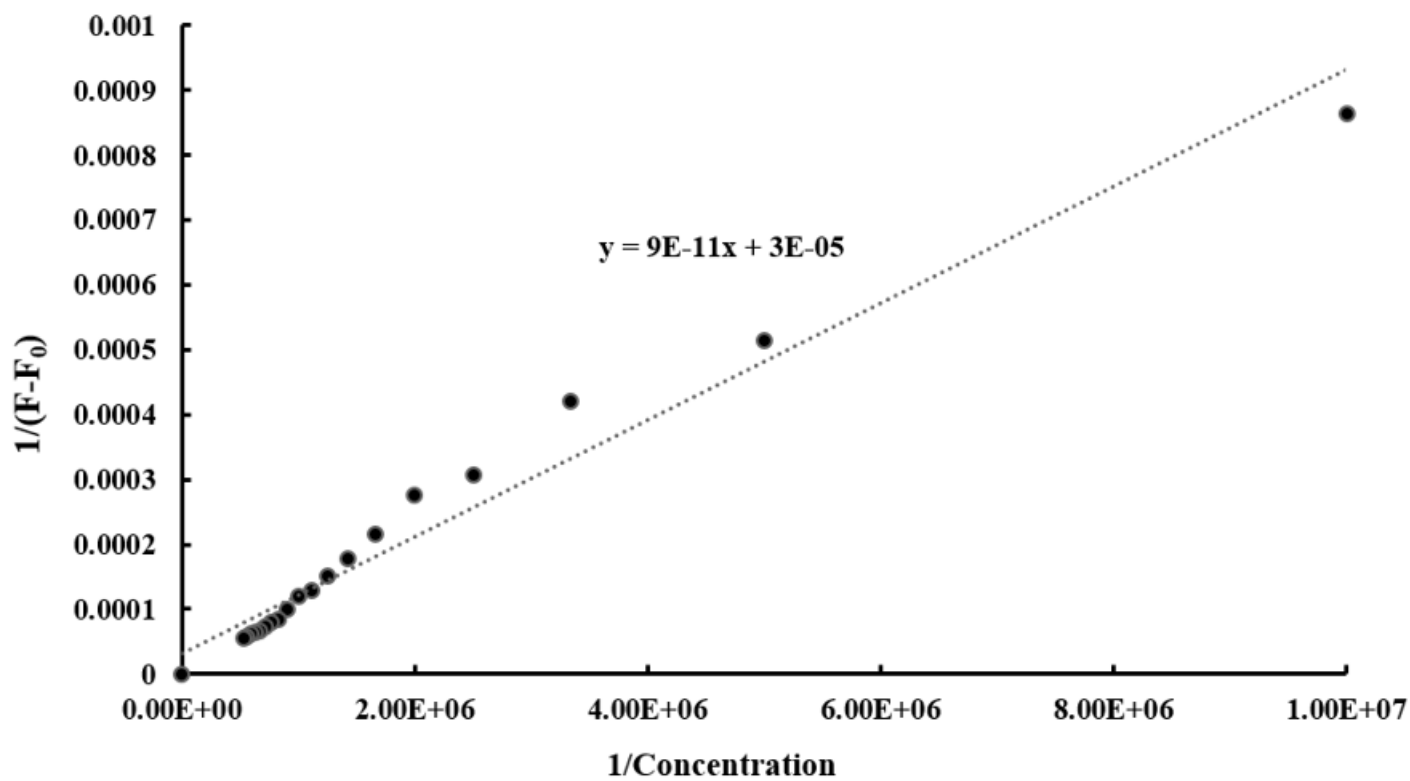
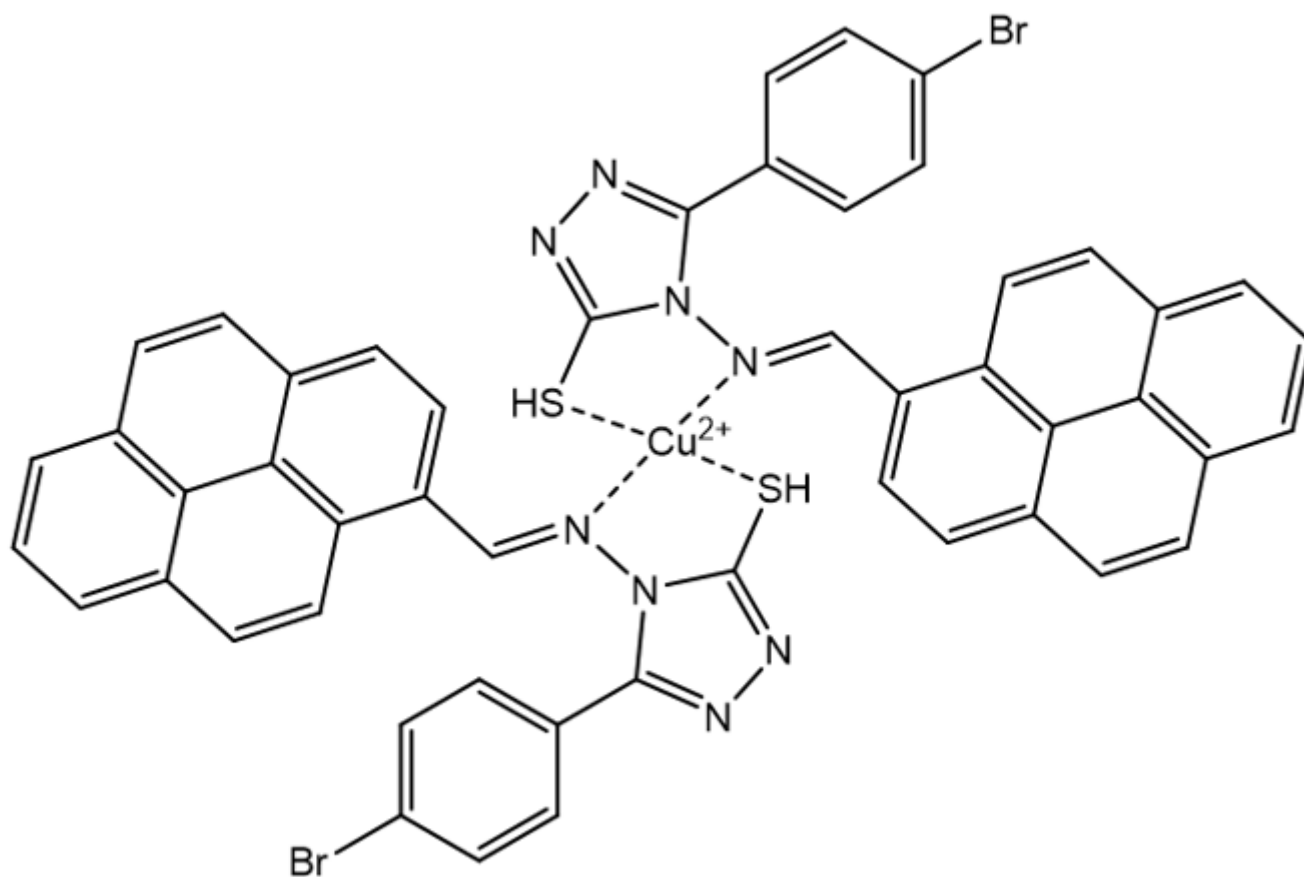


Figure 9

Benesi-Hildebrand graph created by calculating fluorescence intensity for  $\text{Cu}^{2+}$  at 453.1 nm of Probe TP concentration.



**Figure 10**

Proposed coupling structure of Probe TP-Cu<sup>2+</sup>.

## Supplementary Files

This is a list of supplementary files associated with this preprint. Click to download.

- [Schema.png](#)
- [SupportingInformation.docx](#)